Short Communication

Study of Electrical Transport Properties of CZTS/MoSe$_2$/glass Heterostructures

Zhirong Zhang[1], Salma Ikram[2], Adnan Ali[2], Nasir Amin[2], Muhammad Yasir Ali[2], Khalid Mahmood[2*], Kashif Javaid[2], Qurat Ul Ain[3], Nasir Ali[4]

[1]Linfen Vocational and Technical College, Linfen, 041000, China

[2]Department of Physics, Government College University Faisalabad, Faisalabad, Pakistan

[3]Department of Physics, Allama Iqbal Open University Islamabad, Pakistan

[4]Deprtment of Physics, GDC, Saleh Pat, Pakistan

*Correspondence to: Khalid Mahmood, PhD, Associate Professor, Government College University Faisalabad, Allama Iqbal Road, Faisalabad, Punjab, 38000, Pakistan; Email: Khalid.mahmood@lsbu.ac.uk

Abstract

Objective: In this manuscript, we have investigated the temperature dependent electrical transport properties of CZTS/MoSe$_2$/glass heterostructures for solar cell applications.

Methods: MoSe$_2$ coated CZTS diode thin films were fabricated using sol-gel and thermal evaporation methods. During first step, CZTS thin films were grown on glass substrate by sol-gel process and in the 2nd step, MoSe$_2$ thin films were grown on CZTS/glass using thermal evaporation method. The grown structures were post growth annealed at 450-500°C using a muffle furnace.

Results: The structure of each layer was verified by XRD and Raman spectroscopy. SEM analysis has confirmed the smooth surface formation of thin films with a uniform distribution of grains. Electrical properties have been studied by two probe technique after the junction formation between CZTS and MoSe$_2$. Transport properties of the junction showed its semiconductor nature. The resistivity varies from 0 to 7×10^9ohm-cm for the sample annealed at 450°C and varies 0 to 3×10^{10}ohm-cm for the sample annealed at 500°C.

Conclusion: All these parameters made synthesized thin films promising candidates for higher efficiency solar cells, radio modulation and power conversion applications. The effect of the MoSe$_2$ layer on the microstructure and performance of the CZTS film is discussed here in detail. These results serve as guiding principles for preparing high-quality CZTS thin films for potential applications in low-cost solar cells.

Keywords: CZTS/MoSe$_2$ composite, structural analysis, surface morphology, Raman spectroscopy, DC resistivity

1 INTRODUCTION

Innovative R&D to lay on light-trapping system in inorganic thin-film solar cells have been advanced recently. Two dimensional transition metal dichalcogenides based novel ultrathin devices are gaining importance over conventional 3D device because of use of in-plane direction current in their device architectures. The most common of these materials like copper zinc tin sulfide copper zinc tin sulfide (CZTS), copper indium gallium sulfide, and cadmium telluride, which find applications in various electronic and optoelectronic devices such as metal-oxide-semiconductor field-effect transistors, wave shaping, LEDs, harmonic generation, and photovoltaics[1-4]. CZTS-based thin-film solar cells, in particular, are attracting increasing attention for thin-film photovoltaic applications. This is owing to their cost-effective large-scale production, high absorption coefficient of 10^4 cm^{-1}, and efficiency above 30% with average band gap of about 1.5eV. CZTS is a promising p-type material because of its low cost and non-toxic materials compared to others of its kind and is considered potential candidate for 2nd generation solar cells[5].

The performance of thin film solar cell is affected by various factors including film stoichiometric, surfaces plasmonic, thickness hetro/homo junctions and others. The integration of plasmonic layers in photovoltaic devices enhances the optoelectrical properties. For effective light trapping, the layered thin film device such as an n-type layer over p-type CZTS has many advantages including more collection of electron-hole pairs, less quantity of high-quality materials is needed and less energy is used during the fabrication process[6-8]. Moreover, it also reduces the probability of materials losses. All these factors enhance the efficiency of CZTS based solar cells. In view of all this, researchers are doing efforts for making CZTS based solar cells more and more efficient[9,10]. The low open-circuit voltage (Voc) is the most critical impediment to achieving higher efficiencies in CZTS devices compared to the filling factor and short-circuit current density. With this motivation, the effect of $MoSe_2$ layer deposited on CZTS is studied for its enhanced photovoltaic performance.

In electronic devices, $MoSe_2$, inherently n-type material, is a very attractive material to be used as a buffer layer because it provides photon transmission into the absorber semiconductor. For photovoltaics and single junction solar cells the optimal band gap should be ~1.55eV which is closer to band gap values of $MoSe_2$ material[11]. It has large excitons binding energy, non-toxic and low cost materials. To form an ideal p–n junction with CZTS, an appropriate thickness of $MoSe_2$ is needed so that it could give good quantified optical, morphological and electrical properties. It is because thick layer could hinder the transmission of photons and too thin layer could cause shorting due to pinholes in film[12,13]. In current work, $MoSe_2$ coated CZTS diode thin films were grown as layer by layer by sol-gel followed by spin coating and thermal evaporation route. In current study the electrical

properties of $MoSe_2$/CZTS hetrojunction is reported first time. The synthesized diode thin film was further annealed and their temperature dependent charge transport properties were reported.

2 EXPERIMENTAL PROCEDURE

$MoSe_2$ coated CZTS diode thin films were fabricated in three steps. In first step CZTS solution is prepared by sol-gel method. Copper acetate monohydrate, zinc acetate dehydrate, tin chloride, thiourea, 2-methaoxiethanol were used as source materials. All the source materials are alpha grade 99.9% pure. The solutions of all these materials were prepared according to stoichiometric calculations and were mixed together. Zinc acetate monohydrate, copper acetate dehydrate, tin chloride were added into the 2-methaoxiethanol and putt it on magnetic stirrer for an hour at 800rpm and temperature was settled at 50°C the color of the solution was blue before adding the thiourea[14]. After stirring an hour the thio urea was added in the above solution and stirrer for 10 to 20min the color of the solution now changed to light yellow from the blue. In second step, the ultrasonically cleaned substrate was placed set into rotation at 3,000rpm by using spin coater and as prepared solution was spread over the surface of the substrate by micropipette 30s. The sample thus prepared was dried at 28°C for 2-3min[15]. The whole procedure of spin coating was repeated 10 times. The thin film of molybdenum selenide ($MoSe_2$) was prepared on the glass substrate in the evacuated tube by thermal evaporation. At first a test sample of $MoSe_2$ thin films was prepared for phase purity, structural and morphological studies. Highly pure molybdenum and selenide powders were taken according to stoichiometric calculations and are kept in an alumina boat. The source to substrate distance was kept at 12cm and chamber pressure was maintained at 2×10^{-2}Torr[16]. The deposition was made at 500°C. After deposition the sample was cooled to room temperature. In third step, the CZTS thin film coated glass slide was put inside tube furnace and $MoSe_2$ thin film is deposited on it by thermal evaporation by keeping all vacuum parameters same as for test sample of $MoSe_2$. The $MoSe_2$ coated CZTS diode thin film thus prepared was further annealed at 450 and 500°C. The as-grown and annealed samples were characterized by XRD, Raman, SEM techniques for structural and morphological analysis. Electric transport properties of both diode thin films, annealed at 450 and 500°C, were studied by IV measurements using two probe method.

3 RESULTS AND DISCUSSION

Figure 1A shows the XRD scans of CZTS thin film grown by sol-gel method. All the diffraction peaks in the XRD scans of CZTS material thin films is in good agreement with JCPDS card No. 26-0575. Traces of some other phases of SnS and CuS were also observed[17]. XRD diffractograms shown in Figure 1B indicate the pure phase formation of $MoSe_2$ thin film that was deposited by thermal evaporation method[18,19]. The phase purity of as grown CZTS thin film and $MoSe_2$ thin
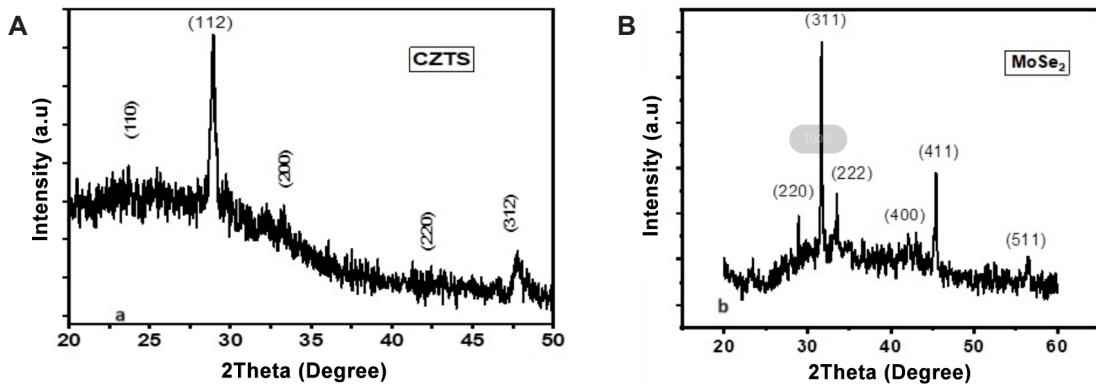
Figure 1. XRD patterns of (A) CZTS thin film synthesized by spin coating and (B) MoSe$_2$ thin film grown by thermal evaporation.
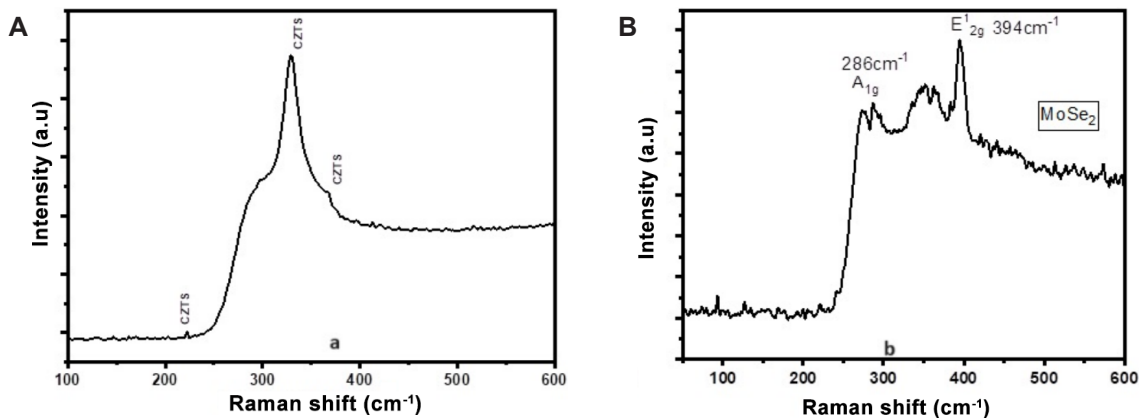

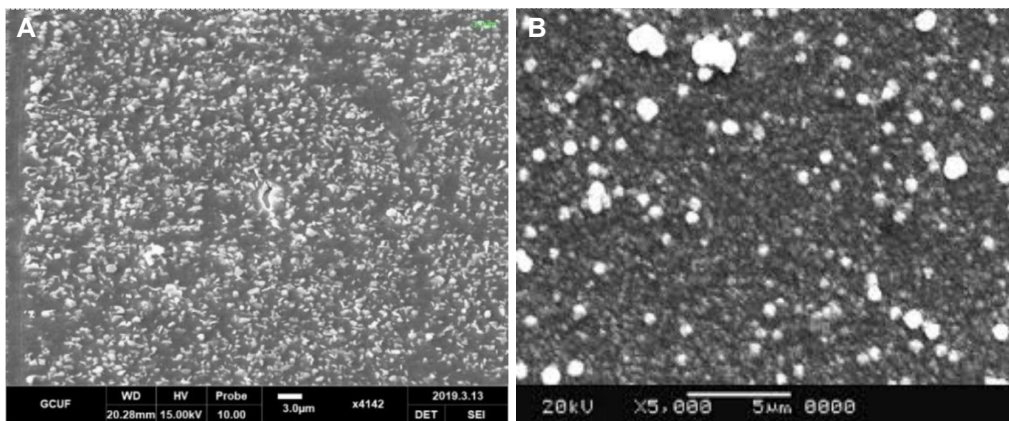Figure 2. Raman spectra of (A) CZTS thin film on glass substrate and (B) MoSe$_2$.

Figure 3. Scanning electron microscopy of (A) CZTS thin film and (B) MoSe$_2$ thin film deposited at 500℃.

films was further verified by Raman spectroscopy. Figure 2A shows the Raman spectra of the CZTS thin film deposited on glass substrate. The characteristic peak of CZTS is identified at 333cm^{-1} and the other peaks are observed at 222cm^{-1} and 37m^{-1} corresponds to CZTS material. Binary and ternary secondary phases of SnS, SnS$_2$, Cu$_2$SnS$_3$, ZnS, Cu$_{2-x}$S, CuS, Cu$_2$S and Cu$_x$S were also observed[20,21]. Figure 2B shows the vibrational modes of the thin film of MoSe$_2$. The Raman profiles exhibited two characteristic phonon modes: One corresponded to the A$_{1g}$ mode (286cm^{-1}) associated with the out-of-plane vibration of Se atoms and the other

corresponded to the E$_{12g}$ mode (394cm^{-1}) associated with the in-plane vibration of Mo and Se atoms. SEM images of both films shows that grains are of comparably equal size and homogenously distributed as depicted in Figure 3A and 3B. MoSe$_2$ thin film surface is smoother than CZTS. These images further shows the good compactness of these thin films[22].

After structural and morphological analysis the electrical carrier transport properties in the annealed CZTS/MoSe$_2$/ Ag junction diode thin films were studied by two probe technique. The temperature is varied from 300 to 800K.
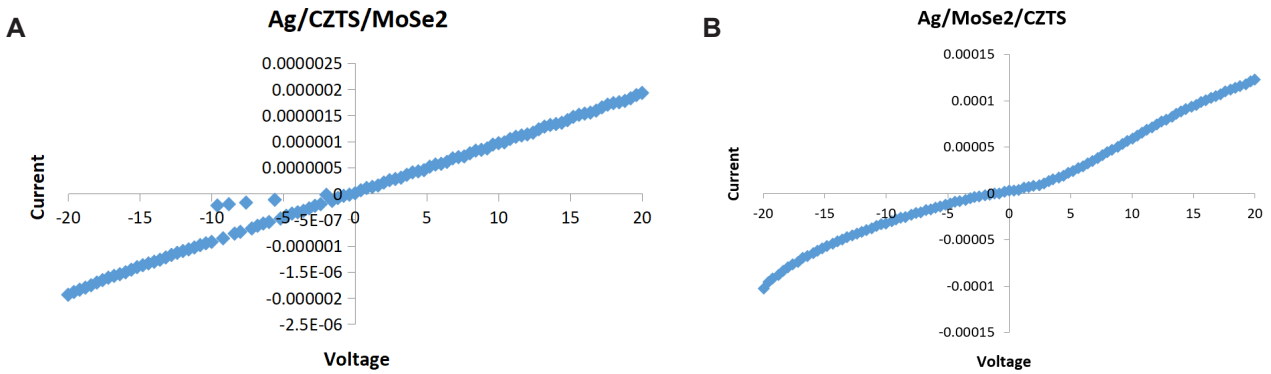
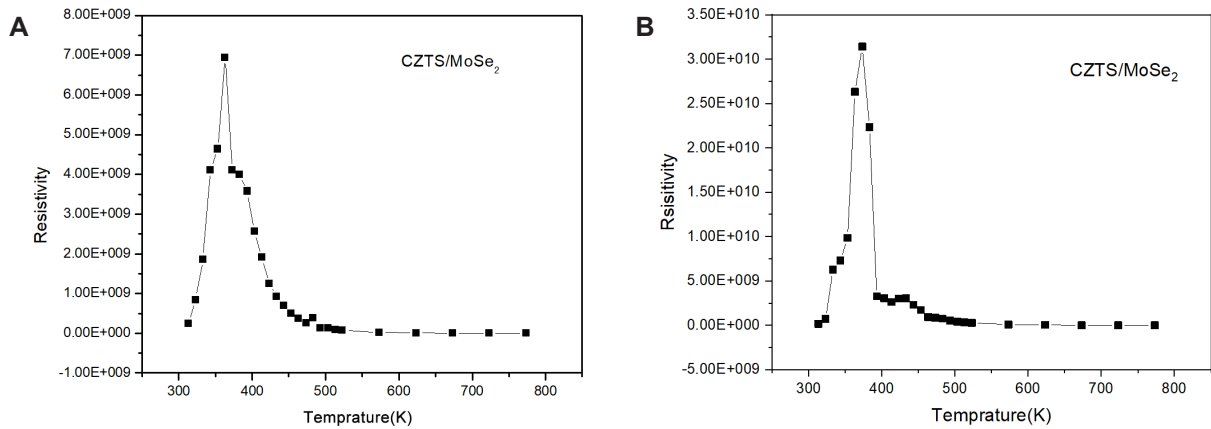**Figure 4. IV characteristics of CZTS/MoSe$_2$ junction annealed at (A) 450℃ and (B) 500℃ with (Ag) contact.**

Figure 5. Resistivity plots of of CZTS/MoSe$_2$ junction annealed at (A) 450℃ and (B) 500℃.

Figure 4A and 4B shows the temperature dependent resistivity graphically. Maximum value of temperature dependent resistivity (ρ) of the materials increases from $7\times10^9\Omega\cdot$cm to $3\times10^{10}\Omega\cdot$cm with increase in annealing temperature. Moustafa M et al[23] used WS$_2$ as buffer layer and observe an enhancement in cell performance to 26.81% Behera N et al[24] studied the electrical properties in vacuum annealed CZTS/Ag multi-layered stack structure of solar cells. They observe a gradual drop in the resistivity is observed with increasing Ag deposition time; however, it is within the tolerable limit of CZTS film. Vigil-Galán O et al[25] also reported the similar results for sprayed Cu$_2$ZnSnS$_4$ thin films growth and its relation with secondary phase formation[25]. In current study both thin film diode samples resistivity of prepared samples firstly increases by increasing the temperature from room temperature to ~363K and then starts decreasing continuously as temperature rises. The value from where the temperature starts decreasing represents Curie temperature of the sample[26-28]. The lower values of resistivity is may be because of nanocrystallinity of thin films. In both annealed and unannealed samples the resistivity of the materials first increases upto temperature ~360K and then decreases at elevated temperatures. The decrease in resistivity is due to transport behavior and some dominating conduction mechanisms like thermionic emissions over grain boundaries barriers reported in other polycrystalline semiconductor thin films in literature. Band tailoring due to junction contributes

to resistivity[29]. Electrons gains additional thermal energy at higher temperatures which may result in their recombination with holes before getting to the depletion region and collecting. The bandgap also may become narrow at elevated temperatures thereby the recombination process of the electrons-holes pair's is accelerated, causing a decrease in resistivity. It may also because of Ag-S bond which is long as compare to the Cu-S bond. This Ag-S bonding may weaker the p-d hybridization than Cu-S resulting in lowering in the valence edge position at higher temperatures.

Figure 5A and 5B depicted that the slop of sample annealed at 450℃ is greater than the sample annealed at 500℃ which indicated the change from ohmic behavior to Schottky-type behavior of junction with rising temperature. The electrical conductivity increases exponentially with increasing temperature (Figure 4A and 4B), hence follows the typical trend for semiconductor thin films[30]. Below 250K, the reverse bias current in both samples is higher than the forward bias current. It is found that conductivity increases with the increase in annealing temperature. Increment in the temperature provides an increase in free volume and segmental mobility. These two entities then permits free charges to hop from one site to another resulting in increase in conductivity. Moreover, the ions could also gain K.E from thermally activated hopping of charge carriers between the trapped sites at elevated temperatures.

4 CONCLUSION

In current studies the junction between the MoSe$_2$ and CZTS formed to study the electrical transport properties. The structural and morphological studies has confirm the successful growth of the desired thin films by the above mentioned route. MoSe$_2$ serves as an excellent window layer by smoothing the device surface and lowering resistivity values. This could result in high transmittance to optimize the light incident on the CZTS absorber layer, as well as serving as a charge transport medium. A distinct conduction region is observed while studying the electric transport properties of the grown diode thin films. Both films exhibit positive dependence of conductivity on temperature, indicating more electrons are excited to the conduction band at elevated temperature. All these parameters made these synthesized thin films promising candidates for higher efficiency solar cells, radio modulation and power conversion applications. The effect of the MoSe$_2$ layer on the microstructure and performance of the CZTS film is discussed here in detail. These results serve as guiding principles for preparing high-quality CZTS thin films for potential applications in low-cost solar cells.

Conflicts of Interest
There is no known conflict of interest.

Author Contribution
Ikram S and Mahmood K started the idea. Yasir Ali M and Zhang Z prepared the samples. Javaid K and Ali A contributed to characterization measurements. Amin N, Ali N and Ain QU contributed to analysis.

Abbreviation List
CZTS, Copper zinc tin sulfide
MoSe$_2$, Molybadnium diselenide

References

[1] Zahra R, Jacob J, Bano N et al. Effect of secondary phases on the thermoelectric properties of Zn$_2$GeO$_4$ nano-crystals grown by thermal evaporation on Au coated Si substrate. *Physica B*, 2019; 564: 143-146.[DOI]

[2] Mahmood K, Samaa BM, Influence of annealing treatment on structural, optical, electric, and thermoelectric properties of MBE-grown ZnO. *J Exp Theor Phys+*, 2018; 126: 766-771.[DOI]

[3] Ikram S, Jacob J, Arshad MI et al. Tailoring the structural, magnetic and dielectric properties of Ni-Zn-CdFe$_2$O$_4$ spinel ferrites by the substitution of lanthanum ions. *Ceram Int*, 2019; 45: 3563-3569.[DOI]

[4] Chowdhury F, Hasan SMF, Alam MS. Morphological and optical properties of vacuum evaporated ZnO thin films. *Turk J Phys*, 2012; 36: 1-7.[DOI]

[5] Ikram S, Jacob J, Mahmood K et al. A Kinetic study of Tb^{3+} and Dy^{3+} co-substituted CoFe$_2$O$_4$ spinel ferrites using temperature dependent XRD, XPS and SQUID measurements. *Ceram Int*, 2020; 46:15943-15948.[DOI]

[6] Ali A, Jacob J, Ashfaq A et al. Al-Othmany, Modulation of structural, optical and thermoelectric properties of sol-gel grown CZTS thin films by controlling the concentration of zinc. *Ceram Int*, 2019; 45: 12820-12824.[DOI]

[7] Huang Z, Zhao L-D. Sb$_2$Si$_2$Te$_6$: a robust new thermoelectric material. *Trends Chem*, 2020; 2: 89-91.[DOI]

[8] Mahmood K, Abbasi S, Zahra R et al. Investigation of large Seebeck effect by charge mobility engineering in CuAlO2 thin films grown on Si substrate by thermal evaporation. *Ceram Int*, 2018; 44: 17905-17908.[DOI]

[9] Mehta C, Saini GSS, Abbas JM. et al. Effect of deposition parameters on structural, optical and electrical properties of nanocrystalline ZnSe thin films. *Appl Surf Sci*, 2009; 256: 608-614.[DOI]

[10] Mahmood K, Jacob J, Shakir M et al. Modulation of thermo-electric properties of GeSeIn thin films by annealing in oxygen environment. *Physica B*, 2019; 572: 66-69.[DOI]

[11] Rehman U, Jacob J, Mahmood K, et al. Direct growth of ZnSnO nano-wires by thermal evaporation technique for thermoelectric applications. *Physica B*, 2019; 570: 232-235.[DOI]

[12] Zaman H, Jacob J, Mehboob K et al. Effect of annealing temperature on thermoelectric properties of zinc nitride thin films grown by thermal evaporation method. *Ceram Int*, 2020; 46: 25992-25995.[DOI]

[13] Tanveer Z, Mahmood K, Ikram S et al. Modulation of thermoelectric properties of thermally evaporated copper nitride thin films by optimizing the growth parameters. *Physica B*, 2021; 605: 412712.[DOI]

[14] Ali A, Jacob J, Arshad MI et al, Enhancement of thermoelectric properties of sulphurized CZTS nano-crystals by the engineering of secondary phases. *Solid State Sci*, 2020; 103: 106198.[DOI]

[15] Ashfaq A, Jacob J, Bano N et al, Tailoring the thermoelectric properties of sol-gel grown CZTS/ITO thin films by controlling the secondary phases. *Physica B*, 2019; 558: 86-90.[DOI]

[16] Rehman A, Jacob J, Zahra R et al. Growth of Mg$_2$GeO$_4$ nano-crystals on Si substrate and modulation of Seebeck coefficient by post growth annealing technique. *Ceram Int*, 2019; 45: 16275-16278.[DOI]

[17] Ashfaq A, Jacob J, Bano N et al. A two step technique to remove the secondary phases in CZTS thin films grown by sol-gel method. *Ceram Int*, 2019; 45: 10876-10881.[DOI]

[18] Singh M, Vijay YK. Preparation and characterization of Zn–Se bilayer thin film structure. *Appl Surf Sci*, 2004; 239: 79-86.[DOI]

[19] Wang Q, Zhang L, Li B et al. 3D interconnected nanoporous Ta$_3$N$_5$ films for photoelectrochemical water splitting: thickness-controlled synthesis and insights into stability. *Sci China Mater*, 2021; 64: 1876-1888.[DOI]

[20] Ammar HR, Sivasankaran S, Alaboodi AS et al. Synthesis, phase evolutions, microstructures, and compaction behavior of four copper-chalcogenide micron-thermoelectric powders (Cu$_2$ZnSnS$_4$/Se$_4$, Cu$_2$MnSiS$_4$/Se$_4$, Cu$_2$MnSnS$_4$/Se$_4$, and

Cu$_2$ZnSiS$_4$/Se$_4$) prepared by mechanical alloying. *Mater Chem Phys*, 2021; 271: 124943.[DOI]

[21] Ashfaq A, Jacob J, Mahmood K et al. Effect of sulfur amount during post-growth sulfurization process on the structural, morphological and thermoelectric properties of sol-gel grown quaternary chalcogenide Cu$_2$ZnSnS$_4$ thin films. *Physica B*, 2021; 602: 412497.[DOI]

[22] Ikram S, Jacob J, Mahmood K et al. Influence of Ce^{3+} substitution on the structural, electrical and magnetic properties of Zn$_{0.5}$Mn$_{0.43}$Cd$_{0.07}$Fe$_2$O$_4$ spinel ferrites. *Physica B*, 2020; 580: 411764.[DOI]

[23] Moustafa M, Mourched B, Salem S et al. Performance enhancement of CZTS-based solar cells with tungsten disulfide as a new buffer layer. *Solid State Commun*, 2023; 359: 115007.[DOI]

[24] Behera N, Mohan DB. Investigation of broad-band optical absorption and electrical properties in vacuum annealed CZTS/ Ag multi-layered stack structure for plasmonic solar cell application. *Opt Mater*, 2022; 127: 112316.[DOI]

[25] Vigil-Galán O, Courel M, Espindola-Rodriguez M et al. Electrical properties of sprayed Cu$_2$ZnSnS$_4$ thin films and its relation with secondary phase formation and solar cell performance. *Sol Energ Mat Sol C*, 2015; 132: 557-562.[DOI]

[26] Ikram S, Ashraf F, Alzaid M et al. Role of nature of Rare Earth ions dopants on Structural, Spectral and Magnetic Properties in Spinel Ferrites. *J Supercond Nov Magn*, 2021; 34: 1745-1751.[DOI]

[27] Ikram S, Jacob J, Mehboob K et al. Role of rare earth metal ions doping on structural, Electrical, magnetic and dielectric behavior of spinel ferrites: A comparative Study. *J Supercond Nov Magn*, 2021; 34: 1833-1842.[DOI]

[28] Mahmood K, Asghar M, Ali A et al. Enhancement of thermoelectric properties of MBE grown un-doped ZnO by thermal annealing. *Adv Energy Res*, 2015; 3: 117-124.[DOI]

[29] Ali A, Cheow SL, Azhari AW et al. Enhancing crystalline silicon solar cell efficiency with Si$_x$Ge$_{1-x}$ layers. *Results Phys,* 2017; 7: 225-232.[DOI]

[30] Najafi N, Rozati SM. Resistivity reduction of nanostructured undoped zinc oxide thin films for Ag/ZnO bilayers using APCVD and sputtering techniques. *Mat Res*, 2018; 21: 1-10.[DOI]